Nanotechnology **20** (2009) 425302 (5pp) doi:10.1088/0957-4484/20/42/425302

The fabrication and characteristics of indium-oxide covered porous InP

D D Cheng[1], M J Zheng[1,3], L J Yao[1], S H He[1], L Ma[1], W Z Shen[1] and X Y Kong[2]

[1] Laboratory of Condensed Matter Spectroscopy and Opto-Electronic Physics, Department of Physics, Shanghai Jiao Tong University, Shanghai 200240, People's Republic of China
[2] School of Materials Science and Engineering, Shanghai Jiao Tong University, Shanghai 200240, People's Republic of China

E-mail: mjzheng@sjtu.edu.cn

Received 15 July 2009, in final form 11 September 2009
Published 25 September 2009
Online at stacks.iop.org/Nano/20/425302

Abstract

Uniform and vertical indium-oxide nanotube (IONT) arrays embedded well in n-type InP single crystal have been successfully prepared *in situ* by porous InP-template-assisted chemical vapor deposition (CVD). This IONT/InP nanostructure reveals high sensitivity to humidity at room temperature, which is ascribed to the ultrahigh surface-to-volume ratio of this nanostructure and the large number of oxygen defected states in IONTs. Such a nanostructure of IONT arrays embedded in a III–V semiconductor substrate could be expected to have potential applications, such as superior gas sensors. This work provides a novel approach for fabricating low-melting metal oxide semiconductor nanotubes.

(Some figures in this article are in colour only in the electronic version)

1. Introduction

In recent years, many groups have actively focused on the synthesis, structure and properties of nanostructured metal oxide semiconductors, such as ZnO [1], SnO_2 [2], Ga_2O_3 [3] and In_2O_3 [4, 5].

Among the existing nanostructured metal oxide semiconductors, indium oxide (In_2O_3), as a very important n-type and wide band gap (direct band gap ~3.6 eV) transparent conducting oxide semiconductor, has stimulated much interest due to its fascinating properties and potential applications in various fields such as opto-electronic nanodevices [6], solar cells [7], gas sensors [8, 9] and DNA detectors [10]. This encouraged us to synthesize high quality In_2O_3 nanostructures for versatile applications. Up to now, In_2O_3 nanostructures, including nanobelts [11, 12], nanowires [13, 14], nanochains [15, 16], nanoparticles [17] and nanotubes [18–20], have been successfully fabricated. In particular, In_2O_3 in nanotube form is expected to be one of the most promising nanostructured materials for chemical sensors, for several reasons. For instance, the nanotubular structure offers a high surface-to-volume ratio. In addition, In_2O_3 possesses enhanced sensitivity and improved response time, which are also advantages to using IONTs as supergas sensors. Various methods, including molecular self-assembly, laser ablation, hydrothermal method, bio-template-based growth and the CVD technique [18–24], have been demonstrated to date for growth of tubular nanostructures.

In this paper we report a simple and novel method to realize the fabrication of ordered IONT arrays embedded well in the semiconductor InP. Here, porous InP has been used as a template and source for *in situ* synthesis of IONT arrays by a CVD technique. Figure 1 presents a schematic illustration of the formation process of IONTs embedded in an InP substrate. The basic approach involves the self-decomposition of a porous InP substrate, a self-provided indium source and nanopore template inducing effects. Indium (from the decomposition of InP) in the nanopores holds oxygen to form In_2O_3 nuclei which deposit on the surface of the pore wall; gradually the IONTs form in the InP nanopores with increasing growth time. This strategy has a few advantages, such as low growth temperature, no need for a catalyst, and direct bonding to the semiconductor substrate. The current–voltage (I–V) characteristics of the IONT/InP composite nanostructure were investigated in different ambient humidities at room temperature. The novel composite nanostructure reveals high-

[3] Author to whom any correspondence should be addressed.

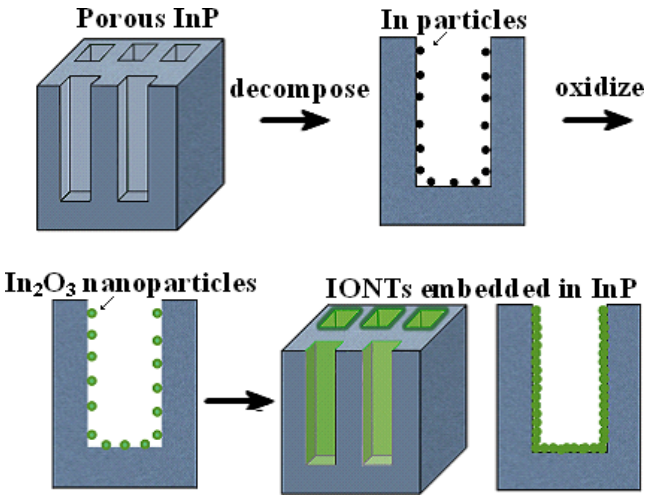

Figure 1. Schematic diagram for the growth process of IONTs embedded in InP.

performance humidity sensitivity in the non-linear part of the I–V characteristics.

2. Experimental details

The IONT/InP composite structure was fabricated as follows. In the first step, porous InP samples were prepared by two-step etching of n-type InP [25]. The electrolyte was a 7.5% HCl aqueous solution. The potential applied on the InP and the anodization time were 8 V and 30 s, respectively. In the second step, the porous samples were annealed for about 50 min in an O_2 atmosphere at temperatures ranging from 400 to 500 °C, in 50 °C steps. The annealing processes were as follows. The porous InP was loaded in a quartz boat as the source material and substrate, and the boat was inserted into a quartz tube. Then the total system was placed into a horizontal electrical resistance furnace, heated up to a set temperature in 30 min and kept at this temperature for about 50 min under a constant flow of oxygen at a rate of 80 sccm (standard cubic centimeters). After that, the substrates were cooled to room temperature. Before being heated, the tube was evacuated for 30 min by a mechanical pump.

3. Results and discussion

Figure 2(a) shows the surface scanning electron microscope (SEM) image of the porous InP. Note there are uniform and straight square pore arrays. The average pore size and the thickness of the sidewall are about 100 nm and 50 nm, respectively. Figure 2(b) displays a SEM image obtained from the sample annealed at 400 °C. The pore arrays still retained excellent periodicity and were extremely straight, compared with the sample without heat treatment (figure 2(a)). It was found that the uniform nanotube arrays embedded well in the semiconductor InP and were formed when the porous InP annealed at 450 °C, as shown in figures 2(c) and (d). However, after being annealed at 500 °C for 50 min, the porous structure of the InP was completely destroyed.

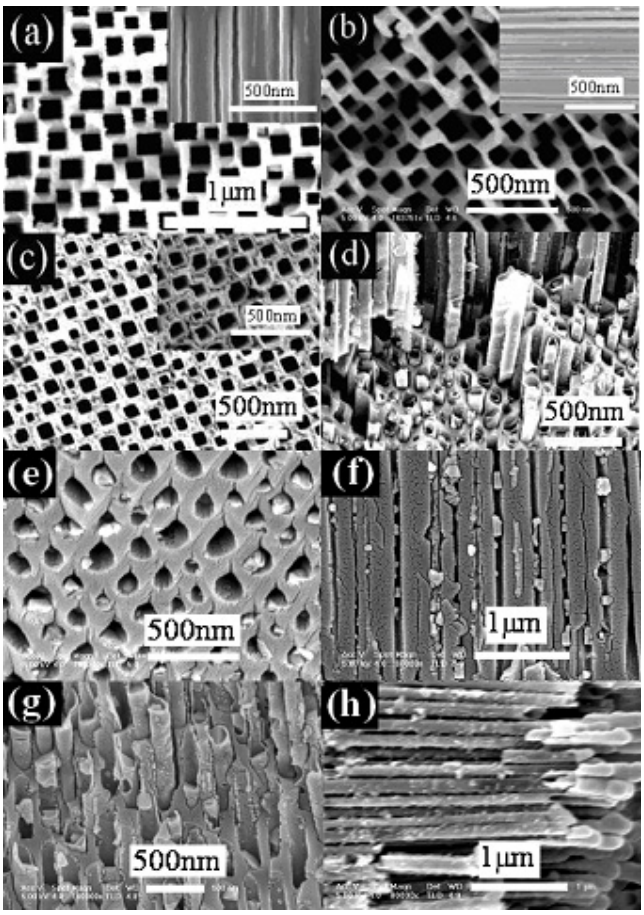

Figure 2. SEM images of porous InP(100) substrate before and after annealing in an oxygen atmosphere under different conditions: (a) no annealing; (b) annealing at 400 °C for 50 min; (c), (d) plane-view and cross sectional image of the porous InP annealed at 450 °C for 50 min, respectively; (e), (f) cross section and longitudinal section SEM images annealed at 450 °C for 5 min; (g) annealing at 450 °C for 15 min; (h) cross section image of the porous InP annealed at 450 °C for 1 h.

The structure and composition of the mentioned nanotubes were examined using x-ray diffraction (XRD). A typical XRD pattern of the sample synthesized at 450 °C in an oxygen atmosphere is shown in figure 3, and all the peaks are indexed to InP and In_2O_3. No other impurity (such as phosphor or indium) peaks were detected. This indicates that the nanotubes formed during the annealing process should be the IONTs.

We suggest that the growth of IONTs in porous InP is based on the vapor–solid model which may involve the following processes. As we know that phosphorus vapor and metal indium vapor were formed by the decomposition of porous InP when the annealing temperature is up to 450 °C [15]:

$$\mathrm{InP(s)} = \mathrm{In(v)} + \mathrm{P(v)}.$$

Subsequently, phosphorus vapor escaped with the atmospheric oxygen and the indium combined with oxygen to form In_2O_3 as given by

$$4\mathrm{In(v)} + 3\mathrm{O_2(g)} = 2\mathrm{In_2O_3(s)}.$$

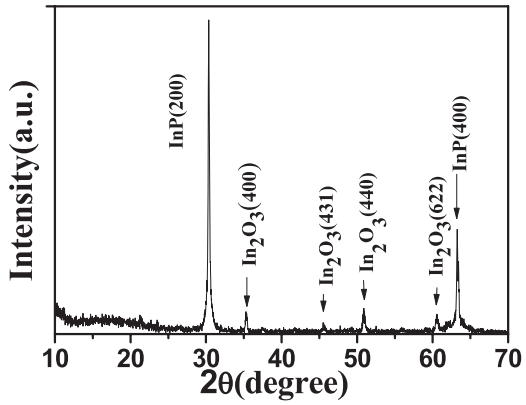

Figure 3. XRD spectrum of nanoporous InP annealed at 450 °C for 50 min in an oxygen atmosphere.

The low-melting point indium (156.6 °C) inside the nanopores was absorbed on the pore wall, and then captured oxygen to form In_2O_3 and directly deposited on the surface of the pore wall. Gradually, the IONTs embedded in nanoporous InP were prepared *in situ* with increasing growth time. The nanotubes are square near the pore top and circular toward the pore, which may be explained by the minimum energy theorem. At the same time, some IONTs peeled off the InP, leaving a gap between the IONT and InP, due to the surface tension of this nanostructure. Oxygen should go through the gap, and the compact InP layer around the IONTs would be decomposed and could be oxidized into In_2O_3 particles that cling to the external tubular wall. Because of the heterogeneous distribution of oxygen in the nanochannels, all the chemical reactions will be accelerated near the pore top. In_2O_3 nuclei preferentially form on the top of the nanopores. Therefore it might be possible to seal the nanotube mouths and some of the IONTs could began to separate with increasing annealing time. To validate above supposition, several more samples were prepared. We set the annealing temperature at 450 °C and the annealing time at 5 min, 15 min and 1 h, respectively; all the other experimental conditions remained unchanged. Figures 2(e) and (f) show, respectively, cross sectional and longitudinal section SEM images taken from the samples annealed at 450 °C for 5 min. Comparing these images with those of porous InP, we observed that the pore wall has been loosened after 5 min and some particles were found on the wall. After 15 min, thin-walled nanotubes were observed and many nanoparticles adhered to the surface of the tube wall, as seen in figure 2(g). On increasing the annealing time to 1 h, the nanotubes began to separate and the nanotube mouths were also gradually sealed (figure 2(h)). By this token, we think that In_2O_3 nucleation would continue on the sealed tube mouth and In_2O_3 nanowires may be obtained along the nanotubes by further increasing the annealing time [15]. Based on the above analysis, this mechanism presages a pathway for the fabrication of other metal oxides semiconductor nanostructures.

The *I*–*V* characteristics of IONTs/InP (porous InP annealed at 450 °C for 50 min in an oxygen atmosphere), as a function of relative humidity (RH) conditions in air, have been recorded at 25 °C. Electrodes were made by connecting copper wires to the surface of nanotube arrays using conducting silver glue. Typical *I*–*V* characteristics of IONTs/InP, measured in the RH range from 92% to 11%, are shown in figure 4(a). In any RH, the *I*–*V* curves of IONTs/InP exhibit linear behavior from −1.5 to 1.5 V and the current values are equal at the same voltage. When the bias voltage is outside this range, the current increased non-linearly with increasing voltage. Marked humidity sensitivity was found in the non-linear part of the *I*–*V* curves. The inset curves in figure 4(a) were obtained from porous InP for comparison. *I*–*V* curves of porous InP basically show no change for different RHs. From the current–RH (*I*–RH) curves (figure 4(d)), when the applied voltage is 2.5 V it is clearly seen that the current of the IONTs/InP increases more quickly at higher RH in air. The *I*–RH curves of porous InP are on the whole horizontal. This shows that indium oxide is responsible for the humidity sensitivity. Figures 4(b) and (c) as a comparison show the measured *I*–*V* curves of porous InP annealed in an oxygen atmosphere for 5 min and in an argon atmosphere for 50 min (other conditions remaining unchanged), respectively. Only at higher RH were changes observed in the *I*–*V* curves for these two samples. For the porous InP annealed in oxygen for 5 min, the current increased more slowly than for IONTs/InP. For the porous InP annealed in argon for 50 min there was a small increase in current at high humidity. This indicates that the *I*–*V* characteristics of annealed porous InP depend on the annealing conditions. The results also mean the IONT/InP nanostructures have good humidity sensitivity.

The sensing mechanism based on defects in the electronic conductivity-based sensing materials could be employed to explain the functioning of In_2O_3-based sensors [26]. For our samples, a large number of oxygen-related defects may be formed during the annealing process based on above analysis of the growth mechanism. We employed photoluminescence (PL) to detect the microstructure characteristic of IONT arrays. Figure 5 (curve a) shows the room-temperature PL spectrum of IONTs/InP. Two peaks at around 520 and 580 nm appeared. For the porous InP (curve b), these PL peaks are very weak. Schlierf *et al* [27] supposed that the PL peaks of porous InP in the range between 520 and 590 nm only result from the oxide composition or some defect states. Zhou *et al* [28] reported a PL peak at 520 nm from In_2O_3 nanoparticles which has been attributed to amorphous In_2O_3, and a 545 nm peak which depends strongly on the effect of oxygen deficiencies. Ko *et al* [29] pointed out a PL peak at 544 nm of the In_2O_3 nanocrystal chains due to recombination between electrons induced by oxygen vacancies and holes. Li *et al* [30] suggested that the PL peak at 593 nm from In_2O_3 nanotubes mainly originates from oxygen deficiencies. According to the above analyses, PL peaks at 520 and 580 nm should be from In_2O_3 nanotubes, which also implies that there are numerous oxygen-relative defects in IONTs. Therefore, when the IONT/InP composite nanostructures are exposed to dry air, oxygen molecules may coordinate into the surface defect sites and trap free electrodes to decrease the carrier density and the mobility of the remnant carriers by creating depletion layers near the surface. With increasing the RH, water molecules in air

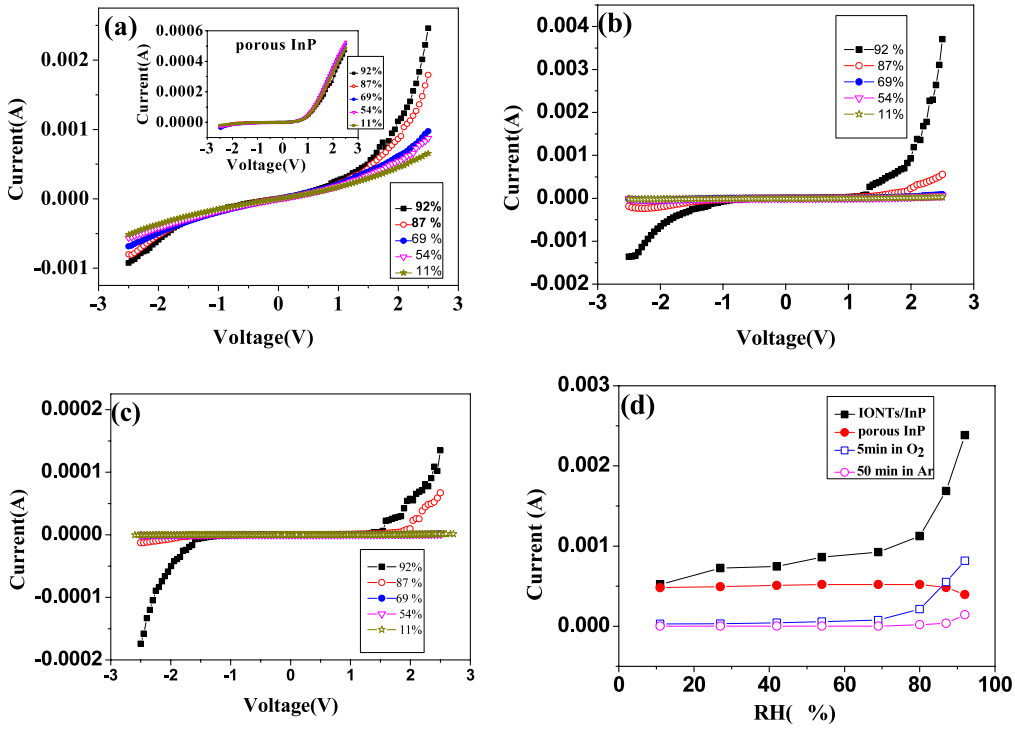

Figure 4. (a) I–V curves of IONTs/InP in the RH range from 92% to 11%. The inset shows I–V curves of porous InP. (b) I–V curves for porous InP annealed at 450 °C for 5 min in an oxygen atmosphere. (c) I–V curves of porous InP annealed at 450 °C for 50 min in an argon atmosphere. (d) I–RH curves of IONTs/InP (■), porous InP (●), porous InP annealed at 450 °C for 5 min (□) and porous InP annealed at 450 °C for 50 min in an argon (○).

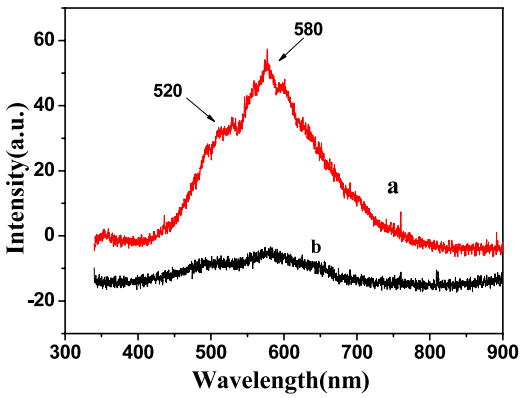

Figure 5. PL spectra of IONTs/InP (curve a) and porous InP (curve b).

coordinate into the surface defect sites of IONTs more easily. Coabsorbed water could change the state of coabsorbed oxygen on semiconductive oxides as reported in the literature [26]. The previously absorbed oxygen and ionized oxygen are replaced by the coabsorbed water molecules. Trapped electrons are liberated by the absorption of water molecules and released to In_2O_3. What's more, the contact clearance between In_2O_3 nanotubes and InP nanopore walls may increase the contact resistance of IONTs/InP, while coabsorbed water in the gap will decrease this resistance. On the other hand, due the large surface-to-volume ratio of the nanotubes, the absorption of oxygen and water molecules changes their conductivity noticeably.

4. Conclusion

In summary, we have developed a novel approach to fabricate ordered IONT arrays inbuilt in porous InP by annealing the porous InP in an oxygen atmosphere. This strategy presented here could be extended to the fabrication of other metal oxide nanotube/III–V semiconductor nanostructures. The sensing mechanism based on defects and large surface-to-volume ratios can be employed to explain the high humidity sensitivity of the IONTs/InP nanostructure at room temperature.

Acknowledgments

This work was supported by the Natural Science Foundation of China (grant no. 10874115), Shanghai Key Basic Research Project of 08JC1411000, Shanghai Nanotechnology Research Project 0952nm01900, and National Major Basic Research Project of 2006CB921507. We thank Instrumental Analysis Center of SJTU for SEM analysis.

References

[1] Tian Z R, Voigt J A, Liu J, Mckenzie B, Mcdermott M J, Rodriguez M A, Konishi H and Xu H 2003 *Nat. Mater.* **2** 821
[2] Kuang Q, Lao C S, Wang Z L, Xie Z X and Zheng L S 2007 *J. Am. Chem. Soc.* **129** 6070
[3] Nogales E, Méndez B and Piqueras J 2005 *Appl. Phys. Lett.* **86** 113112
[4] Guha P, Kar S and Chaudhur S 2004 *Appl. Phys. Lett.* **85** 3851

[5] Singh N, Zhang T and Lee P S 2009 *Nanotechnology* **20** 195605
[6] Cui Y, Lieber C M, Young I R, Larkman D J, Gilderdale D J and Hajnal J V 2001 *Science* **291** 851
[7] Miller A J, Hatton R A, Chen G Y and Silva R S P 2007 *Appl. Phys. Lett.* **90** 023105
[8] Zeng Z M, Wang K, Zhang Z X, Chen J J and Zhou W L 2009 *Nanotechnology* **20** 045503
[9] Zhang D H, Liu Z Q, Li C, Tang T, Liu X L, Han S, Lei B and Zhou C W 2004 *Nano Lett.* **4** 1919
[10] Li Z, Chen Y, Li X, Kamins T I, Nauka K and Williams R S 2004 *Nano Lett.* **4** 245
[11] Pan Z W, Dai Z R and Wang Z L 2001 *Science* **291** 1947
[12] Comini E, Faglia G and Sberveglieria G 2002 *Appl. Phys. Lett.* **81** 1869
[13] Zheng M J, Zhang L D, Li G H, Zhang X Y and Wang X F 2001 *Appl. Phys. Lett.* **79** 839
[14] Zeng F H, Zhang X, Wasng J, Wang L S and Zhang L 2004 *Nanotechnology* **15** 596
[15] Zhong M, Zheng M J, Zeng A S and Ma L 2008 *Appl. Phys. Lett.* **92** 093118
[16] Ko T S, Chu C P, Chen J R, Chang Y A, Lu T C, Kuo H C and Wang S C 2007 *J. Vac. Sci. Technol.* A **25** 1038
[17] Murali A, Brave A, Leppert V J and Risbud S H 2001 *Nano Lett.* **1** 287
[18] Li Y B, Bando Y and Golberg D 2003 *Adv. Mater.* **15** 581
[19] Zhong M, Zheng M J, Ma L and Li Y B 2007 *Nanotechnology* **18** 465605
[20] Du N, Zhang H, Chen B D, Ma X Y, Liu Z H, Wu J B and Yang D R 2007 *Adv. Mater.* **19** 1641
[21] Chun H J, Choi Y S, Bae S Y and Park J 2005 *Appl. Phys.* A **81** 539
[22] Cheng B and Samulski E T 2001 *J. Mater. Chem.* **11** 2901
[23] Wei A, Sunb X W, Xu C X, Dong Z L, Yu M B and Huang W 2006 *Appl. Phys. Lett.* **88** 213102
[24] Zhang X H, Zhang Y, Xu J, Wang Z, Chen X H and Yu D P 2005 *Appl. Phys. Lett.* **87** 123111
[25] Zeng A S, Zheng M J, Ma L and Sheng W Z 2006 *Nanotechnology* **17** 4163
[26] Travesa E 1995 *Sensors Actuators* B **23** 135
[27] Schlierf U, Lockwood D J, Graham M J and Schmuki P 2004 *Electrochim. Acta* **49** 1743
[28] Zhou H, Cai W and Zhang L 1999 *Appl. Phys. Lett.* **75** 495
[29] Ko T S, Chu C P, Chen J R, Chang Y A, Lu T C, Ku H C and Wang S C 2007 *J. Vac. Sci. Technol.* A **25** 1038
[30] Li Y, Bando Y and Golberg D 2003 *Adv. Mater.* **15** 581